Forensic Engineering Technique for Analysis of an Explosion Incident

Ganchai Tanapornraweekit

ganchai@siit.tu.ac.th

Sirindhorn International Institute of Technology

Thimira Abeysinghe

Thiita Designers & Consultants Pvt. Ltd.

Somnuk Tangtermsirikul

Sirindhorn International Institute of Technology

Research Article

Keywords: Blast loads, Concrete structures, Damage assessment, Fragment, Forensic engineering, Lethal zone

Posted Date: October 20th, 2023

DOI: https://doi.org/10.21203/rs.3.rs-3436701/v1

Additional Declarations: No competing interests reported.

Forensic Engineering Technique for Analysis of an Explosion Incident

Abstract

This article investigates the validity of current forensic practices to analyze an explosion event. The real explosion incident at Erawan shrine in central Bangkok on August 17, 2015 is selected as a case study. By comparing the structural damage at the blast site to that obtained from FE analyses, an equivalent bare charge weight of TNT used in the incident can be estimated. It is found that an equivalent bare charge TNT weight of 3 kg could possibly be used for the bomb. Furthermore, the cased charge weight can be calculated based on the equivalent weight of bare TNT charge. To confirm the validity of the calculated explosive weight, a combined lethal zone from blast pressure and scattered fragments was analysed. Human damage from blast pressure is analysed based on the Bowen's lethality curves. Lethality zone from exploded fragments is drawn based on a 50% probability of lethality which considers hit density and kinetic energy of fragment. The analysed lethal zone agrees reasonably well with the actual observed damage level. With the proposed forensic engineering technique, the management and policies for homeland security can be improved for a safer community.

Keywords: Blast loads; Concrete structures; Damage assessment; Fragment; Forensic engineering; Lethal zone

1. Introduction

Currently, terrorist bombs have occurred worldwide. In Thailand, bomb blast attacks in the south border part of the country, however, such an occurrence has now reached major city centers. The blast on August 17, 2015 at Erawan shrine in the center of Bangkok is the most recent terrifying incident. Forensic engineering is an application of engineering knowledge to investigate failure or other performance problems. Sometimes, forensic engineering also involves finding of evidences for support of lawsuit [1]. This article aims to use forensic engineering techniques to analyse an explosive weight used in a bombing incident and later predict a lethal radius caused by blast pressure and a lethal zone caused by fragment impact.

The analysis of explosion at Erawan shrine is presented in this paper as a case study of using forensic engineering techniques to analyse bomb blast events. All accessible evidences left at the incident scene were implemented into each steps of analysis. Analysis performed in this study is kind of reverse analysis by comparing the damage levels of nearby structures and lethality of humans in the incident to those from analysis results. The forensic engineering techniques used in this study compose of using a finite element method (FEM) to analyse the damage levels of structures under explosion, using an analytical calculation and Bowen's lethality curves to analyse lethality zone of humans resulted from blast fragments and pressure. Analysis results in this article

provide some insight of evidence to concerned authorities. It is noted that this paper does not intend to specify type of explosive material used in this incident as it should be examined through the chemical compositions left at the explosion site and it is considered outside the scope of this article.

2. Theoretical background

2.1 Structural damage

Blast load causes structure to vibrate until the effects of the blast load dissipate. Global (bending) and local (shear, spalling and scabbing) responses can be observed in a structure subjected to blast load [2], [3]. Bending of structural member will impose deformation/distortion of the member. Such distortion causes flexural and shear cracks as observed by [3]-[12]. Furthermore, concrete on the incidence face maybe damage from the blast. This phenomenon is known as scabbing [3]. Ejection of concrete debris from the opposite face of the structure where the blast load impacts is known as spalling [3], [13]. This is a crucial mode of failure as ejected debris may cause injury to people and/or damage to equipment where the structure is intended to protect. Higher explosion may cause spalling to occur from the opposite face and propagate o the incident face which is known as breaching. In case of breaching in the main structural members such as column or shear wall, it may cause structure to collapse. Both scabbing and spalling may manifest in case of close-in detonation [3] and it is important to identify these different failure modes to minimize or prevent them from occurring. Such behaviour of reinforced concrete structures were reported in [6], [12], [14] through means of test and finite element (FE) analyses. Due to bending and vibration of concrete panels under such explosion, flexural cracks can be observed also from front and rear faces of structure.

Designs methods used in current practice are mainly based on Single Degree of Freedom (SDOF) approach [15]. SDOF is an analysis procedure which was introduced by [16] where the total system is transformed to a lump mass with equivalent spring stiffness. However, reliable predictions may be difficult to achieve due to complex material responses under blast loads [15], [17], [18]. It is noted that SDOF can only predict displacement-time history of blast loaded structure. Failure modes cannot be predicted using SDOF analysis.

Based on experimental observations, a chart used to predict types of damage of concrete panels subjected to blast loads was presented in [13] by considering panel thickness, explosive weight and standoff distance. Three levels of damage presented in the chart are no damage, spalling and breaching. However, effects of steel reinforcement are not considered for the damage prediction. Apart from the costly real blast tests, numerical simulation is a very useful tool to quantify responses and failure modes of structures more reliably. Due to the advancement of computers and computational mechanics, many commercial software packages have been introduced and widely utilized to perform numerical simulation of concrete structures under blast loads. In

addition, a computer aided numerical simulation is able to provide more information for blast loaded structures which may be difficult to trace from the blast tests [15]. LS-DYNA [19] is one of a commercial software widely used to simulate structural responses under blast loading [6],[11],[12],[14],[15],[20]. Concrete_Damage_Rel3 (MAT72R3) was utilized in [6],[11],[12],[14],[20] to model an ordinary concrete. MAT72R3 was developed based on [21] which is a modification from [22]. This model allows users to implement their user defined dynamic increased factors (DIFs) as one of inputs. MAT72R3 is considered to be well suited to simulate concrete subjected to blasts loads [12],[23],[24].

In some cases of finite element modeling, it was reported that high blast pressure may cause severe mesh distortion, forcing the simulation to produce inaccurate results and/or terminate prematurely [11],[12],[18]. This is solved by utilizing suitable opted erosion criteria to delete elements with unrealistically large deformation. In addition, a proper strain-based erosion algorithm can be employed to simulate concrete cracks [15]. Concrete cracks on the front and rare surface as well as spall damage were simulated using erosion algorithm in [10]. Furthermore, with properly adopted erosion algorithm, a punching failure due to contact detonation was accurately simulated in [12]. It is noted that a complete break up of concrete can be simulated using an erosion algorithm as well [25]. Erosion criteria based on maximum principal strain were employed in [25], whereas criteria based on both tensile strength and maximum principal strain were considered by [26]. After employing different erosion criteria, [10] suggested to use a maximum principal tensile strain-based criteria to simulate more realistic results.

2.2 Injury and lethality

From a bomb explosion, injury and lethality may occur from blast pressure itself and from flying fragments. The following sections discuss this occurrence and explain the procedure to obtain the lethal zone of a bombing incident.

2.2.1 Damage from blast pressure and impulse

A person will be subjected to different possibility of injury levels based on the intensity of blast pressure and impulse which is the effect combined between blast pressure and duration of the explosion. In order to evaluate the human lethality from explosion, the Bowen lethality curves [27] which consider both blast pressure and duration of explosion are employed in this research.

Bowen considers the possibility of lethality differently between the cases of people standing in an open field, near reflecting wall and in a prone position. Since the blast incident at Erawan shrine was in the open field, the lethality curves for open field scenario is chosen for the analysis in this paper. There are four curves where each curve corresponds to injury threshold, 1% lethality, 50% lethality and 99% lethality. The curves are plotted between blast pressure and

duration of blast positive phase. Each pair of pressure and duration of blast on each curve corresponds to the same level of probability of lethality.

2.2.2 Damage from fragments

Apart from blast pressure, another threat which affects damage levels of person is fragments produced during the explosion. Fragments can be generated when the explosive material is packed in the container or casing similarly to a pipe bomb. The container will be torn apart into pieces of fragments during an explosion. This type of fragment has been known as natural (primary) fragment which is irregular in shape and size. In some cases, a number of preformed fragments are intentionally filled between the explosive and the inner surface of explosive casing. Generally, steel balls are used as preformed fragments where they can be packed densely to maximize the number of fragments in the bomb. Once the bomb explodes, these two types of fragments will be ejected with speeds higher than supersonic causing high damage to surrounding structures and injury to proximate population.

It should be noted that not all the fragments are capable to cause damage. They should possess an adequate amount of kinetic energy which depends on their mass and residual velocity before striking target. From the results of [28], it was observed that the distribution of weight and number of natural fragments follow Mott's distribution in accordance with Equation 1 and Equation 2.

$$N(m) = \frac{M_0}{2M_k^2} e^{-\left(\frac{m^{1/2}}{M_k}\right)} \tag{1}$$

$$M_k = Bt^{5/6} d^{1/3} \left(1 + \frac{t}{d}\right) \tag{2}$$

where m is mass of fragment, $N(m)$ is number of fragments of weight higher than m, M_0 is mass of casing, M_k is distribution factor, B is a constant based on types of explosive and materials of casing, t and d are thickness and inside diameter of casing.

The initial velocity of a fragment can be calculated from the Gurney's equation [29] shown in Equation 3.

$$V = \sqrt{\frac{2E}{\frac{M}{C} + \frac{1}{2}}} \tag{3}$$

where V is initial velocity of the fragment, $\sqrt{2E}$ is a Gurney constant for a given explosive, C and M is the weight of explosive and casing, respectively. It is noted that the difference in the initial velocity of natural and preformed fragments is resulted from gas leakage between preformed fragments. [29] suggested to reduce the C/M value to represent the greater energy loss until acceptable agreement between the calculation and the test data was achieved. This research adopts the gas reduction factor of 0.50 as suggested in [29].

In order to determine the kinetic energy of fragment, the velocity of fragment when it strikes target has to be evaluated. However, the velocity obtained from Equation 3 is an initial velocity of the fragment when it is ejected. The reduction of fragment velocity due to drag force has to be considered and can be calculated using Equation 4 [30].

$$ln\left(\frac{V_s}{V}\right) = -\frac{C_D A_f \rho_a s}{2m} \tag{4}$$

where V_s is velocity of fragment at distance s, V is initial velocity of the fragment, C_D is drag coefficient, A_f is surface area of the fragment, ρ_a is air density, s is distance travelled by the fragment and m is mass of the fragment.

In addition to velocity of fragment, direction of fragment or spray angle (θ) has to be considered to assess the lethal zone as well. The angle can be calculated using an equation proposed by Shapiro [31] which is shown in Equation 5 where V stands for initial velocity of the fragment, V_0 is detonation velocity of the explosive, ϕ_1 is curvature of the pipe bomb shell, and ϕ_2 is its position compared to the detonation point.

$$tan\,\theta = \frac{V}{2V_0} cos(\frac{\pi}{2} + \phi_2 - \phi_1) \tag{5}$$

A person will be injured if there is at least 1 fragment fired into a vulnerable surface area of the person which is around 0.5 m^2 [32]. In other words, a fragment hit density of 2 fragments/m^2 is a minimum criterion to injure a person. This criterion can be used to draw a lethal zone resulted from blast fragment. A person who stands inside this area will be definitely hit by at least 1 fragment. However, there is also possibility to be hit if a person stands outside the lethal area.
In addition to the fragment hit density, kinetic energy of the fragment must be considered in order to determine a probability of lethality. Probability of lethality (P_l) can be calculated from Equation 6 where N_{hits} is hit density of fragments and $P_{l|hit}$ relates to kinetic energy of fragment, type of target and damage level to the target. Threshold levels of $P_{l|hit}$ are shown in Table 1. The criterion used to define the boundary of the lethal zone is a 50% probability of lethality as stated in [33].

$$\begin{aligned} P_l &= 1 - \left(1 - P_{l|hit}\right)^{N_{hits}} && \text{for } N_{hits} > 1 \\ P_l &= N_{hits} P_{l|hit} && \text{for } N_{hits} < 1 \end{aligned} \tag{6}$$

Table 1. Values of $P_{k|hit}$ for different damage levels on three types of targets [33]

Type of target	Kinetic energy of fragment that causes different levels of damage, (kJ)		
	Light damage (P_k = 0.1)	Moderate damage (P_k = 0.5)	Heavy damage (P_k = 0.9)
Person	0.1	1	4
Airplane	4	10	20
Armored vehicle	10	500	1,000

3. Case study

3.1 Weight of explosive used in the bombing at Erawan shrine, Bangkok

In order to investigate the weight of explosive used in the incident at Erawan shrine, one of the obvious evidences to be used in the forensic analysis is the damage level of the reinforced concrete (RC) column fence and slab of the shrine. It was shown by online news media [34] that the column was subjected to a massive damage due to the bombing as presented in Figure 1. Bending of column, concrete spalling in both column and slab and tearing of steel fence were observed. Since the area clean up and repair work of the RC fence and slab were finished by the next morning after the incident, the authors' team did not have a chance to investigate and collect the evidences in time. In addition, there is no more detailed evidence of this incident on published data except those from news medias referred in this article.

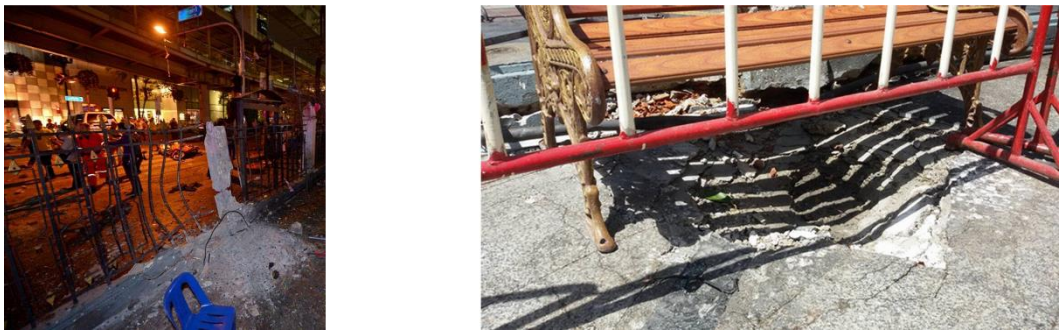

Figure 1 Damage level of RC fence column and RC slab (photos from [34] and Than Tao Mahaprom Foundation)

A series of analyses were performed using an explicit FE code LS-DYNA [19] in order to investigate responses and damage levels of the fence structure. This study employs FE analysis to investigate responses of fence structure subjected to explosion from different explosive weights. The analyzed responses and failure patterns of the structure are compared with that resulted from the real explosion as shown in Figure 1. Each analysis differs in explosive weight. The analysed damage levels are then compared with the actual damage level observed from the blast site. The possible weight of explosive used in the incident can then be evaluated. Two possible explosive materials, TNT and C4 are employed as analysis examples. In case of other types of explosive, most of their TNT equivalencies are larger than that of TNT but lower than that of C4 [35]. Therefore, only these two explosives are considered for analyses.

The dimensions of the fence structure were measured after the blast incident. The dimension of a square column section is 250×250 mm including 25 mm of finishing mortar on each surface. Four deformed bars (DB) with a diameter of 12 mm were detected at a distance approximately 55 mm from the column surface using a cover meter. Stirrups of the column were also detected by a cover meter and they are round bars (RB) with a diameter of 6mm @150 mm. Generally, the structural response obtained from FE analysis is mesh dependent. Therefore, the

mesh sensitivity analysis was performed by varying the mesh size from 20 mm, 10 mm and 5 mm. It was found that the damage pattern of 10 mm mesh model similar to that of 5 mm mesh model, however, much time consuming is required to finish the analysis of 5 mm mesh model. Therefore, the 10 mm mesh model was adopted for the analysis shown in this article.

The compressive strength of concrete and mortar used in the analysis are 24 MPa and 10 MPa, respectively. MAT_CONCRETE_DAMAGE_REL3 (or MAT 72R3) was used to model concrete in the analysis. The analyses in this study adopt the automatic parameter generation of MAT 72R3 to model concrete for RC fence and RC slab of the shrine. The tensile strength of DB12 and RB6 are 500 MPa and 360 MPa, respectively. MAT_PIECEWISE_LINEAR_PLASTICITY was used to model all the steel rebars. The strain rate effects based on Crawford and [36], and [37] were also implemented in material constitutive laws of both concrete and steel rebars.

Three FE models were analyzed with three different explosive weights which are 2 kg, 3 kg and 4 kg for each FE analysis case. The model analyzed in this study is presented in Figure 2.

TNT was initially selected to be the explosive used in the model as it is the standard type of explosive which has reliable explosion energy and normally used as a reference in the design of structures under blast loading [35]. The explosive was initially assumed to be a bare TNT charge. Based on the observation of video clip from surveillance camera and also the damage pattern shown in Figure 1, the bomb was placed under the bench where the distance from the center of the bench to the fence was measured to be approximately 0.30 m from the fence structure. Since the bomb exploded on ground, it is considered to be a hemi-spherical surface burst [35] where reflection of the blast wave from ground reinforces the original blast waves. The blast pressure-time histories applied to all the FE models in this study were generated using the keyword *LOAD_BLAST_ENHANCED in LS-DYNA. The blast option 1 in this keyword was selected to represent a hemispherical surface burst.

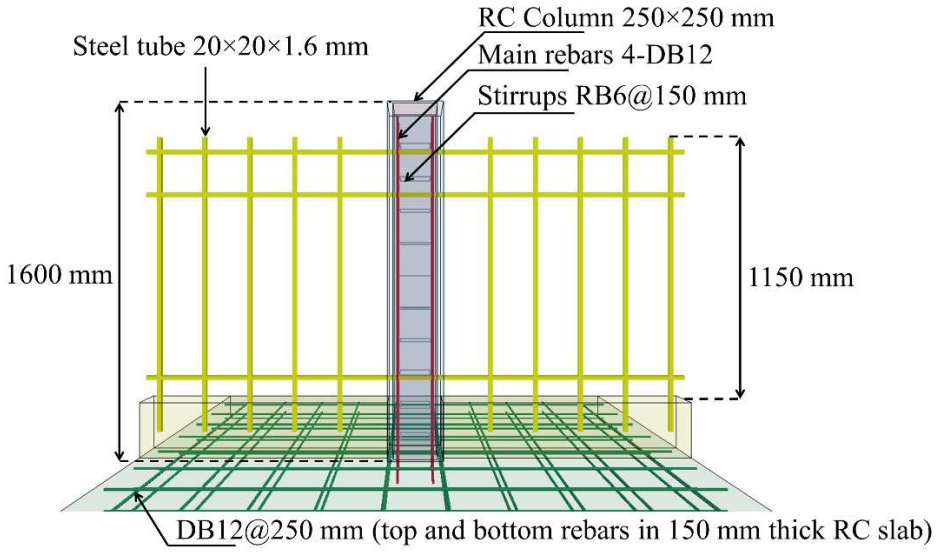

Figure 2 FE Model of the RC fence column and RC slab

Figure 3, Figure 4 and Figure 5 show damage levels of the fence structure and RC slab resulted from explosion of 2 kg, 3 kg and 4 kg of bare TNT charge, respectively. These damage levels were compared with the damage level observed at the scene of incident (see Figure 1).

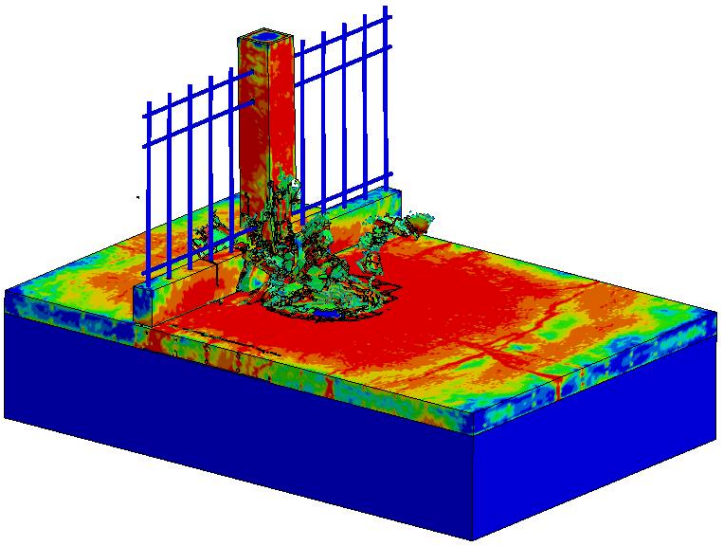

Figure 3 Damage level of structure caused by an explosion of 2 kg of bare TNT charge

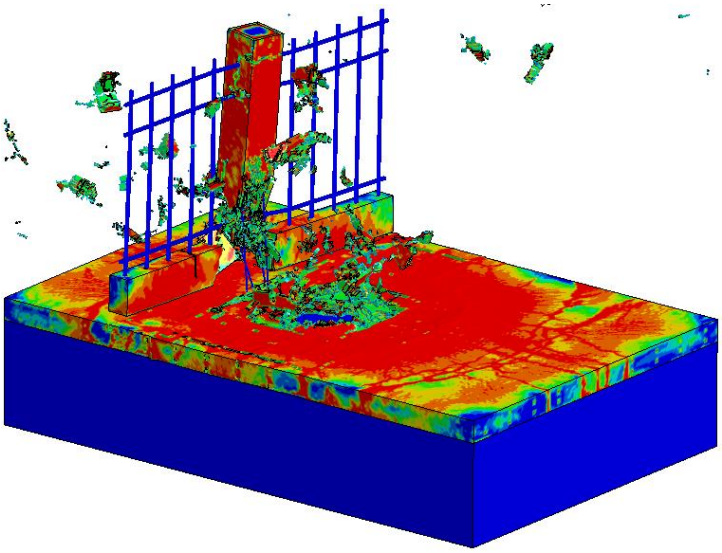

Figure 4 Damage level of structure caused by an explosion of 3 kg of bare TNT charge

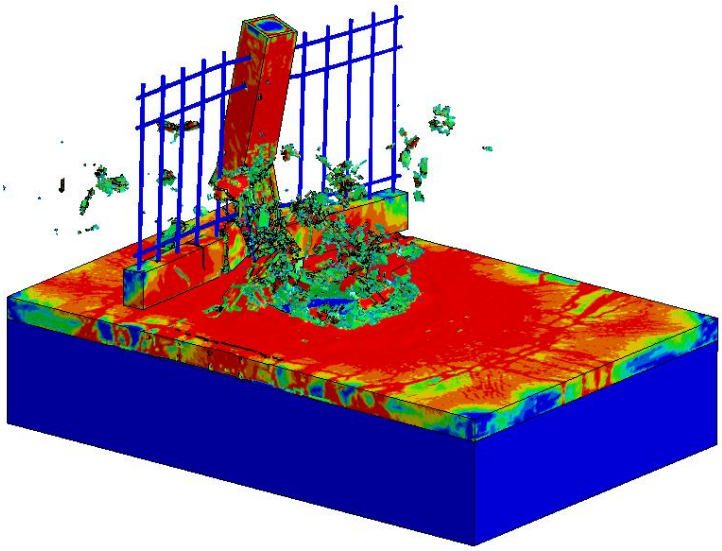

Figure 5 Damage level of structure caused by an explosion of 4 kg of bare TNT charge

All the analysis cases show spalling of the concrete slab at the position of explosion. The damage level of reinforced concrete slab resulted from the explosion of 3 kg of bare TNT is comparable to that observed at the blast site (see Figure 1 and Figure 4). Area of concrete spalling on the slab from the analysis of 4 kg of TNT is much larger than that of the actual incident. The damage levels of the concrete column are also different in each analysis case. Concrete spalling in the column was observed in all analysis cases, i.e. 2 kg, 3 kg and 4kg of TNT. The severity of concrete spalling increases once the weight of TNT increases to 3 kg and 4 kg. The damage level of column subjected to the explosion of 4 kg of TNT is higher than the actual damage level. The base of concrete column in the real blast incident was still intact whilst the analysis of the explosion from 4 kg of TNT shows that it is totally destroyed. Position and amount of concrete spalling of the column from the analysis case of 3 kg of TNT explosion agree rather well with that of the actual damage level. It is worth noting that the keyword LOAD_BLAST_ENHANCED is employed to simulate the blast pressured applied on the planar surfaces of the structures. Therefore, this load function will not be applied to the steel fence which was modeled using beam elements.

In summary, the simulated damage level of the fence column and slab resulted from the explosion of 3 kg TNT is comparable to that observed from the real incident. Therefore, the weight of the explosive used in the incident is equivalent to about 3 kg of bare TNT charge.

3.2 Equivalent explosive weight in the pipe bomb

News media [34], [38] reported that many fragments made of galvanized steel were found at the crime scene. Therefore, it is apparent that the explosion in this incident was resulted from the detonation of pipe bomb where the explosive was filled in the galvanized steel casing. Further analysis was performed to determine the possible dimension of pipe bomb and weight of cased charge which is equivalent to 3 kg of bare TNT charge obtained from the FE analyses.

According to [39], blast pressure produced by the detonation of explosives inside a casing or pipe bomb is different from that of bare charge explosion. Relation between bare and cased charges which produce the same level of blast pressure is shown in Equation 7 where C_b, C, M and f are weight of bare charge, weight of cased charge, weight of metal casing and a factor based on material of casing and type of explosive, respectively. The value of f for steel casing and TNT is 0.46. In case of pipe bomb, some energy is required to burst the casing. Therefore, the weight of cased charge required to produce the same level of blast pressure is usually higher than the weight of bare charge.

$$\frac{C_b}{C} = \left\{ (1-f) + \frac{f}{1+2\left(\frac{M}{C}\right)} \right\} \tag{7}$$

This section was aimed to analyze and estimate possible sizes of the pipe which was used to pack the explosives. Figure 6 shows the captured photo of the criminal with his backpack. Unfortunately, this captured photo from the surveillance camera is the only available photo of the criminal captured in the scene of incident. The length of the pipe which can be put in the backpack should be in between 200 to 300 mm. The pipe length was assumed to be 250 mm for analyses in this study. The case studies reported in this article were limited to two types of explosives which are TNT and C4 where their densities are 1,630 and 1,600 kg/m^3, respectively. The pipe sizes which can be fitted into the backpack and widely available in stores are 80 mm, 100 mm with 125 mm in diameter. As given in Table 2, pipe diameters of 80, 100 and 125 mm with 250 mm in length can be used to pack 1.58 kg, 2.87 kg and 4.49 kg of TNT, respectively. It should be noted that these weights of explosive are calculated based on the remaining volume after the steel balls are distributed on the inner surface of the pipe and around the explosive. These TNT cased charge weights were converted to equivalent TNT bare charge weights using Equation 7. The equivalent TNT bare charge weights are 1.09 kg, 2.04 kg and 3.15 kg for the pipe diameter of 80, 100 and 125 mm, respectively as presented in Table 2.

Figure 6 Criminal with his backpack captured by surveillance camera (photo from [40])

Table 2. Summary of the possible dimensions and weights of pipe bomb

Pipe diameter (mm)	Thickness (mm)	Weight of steel pipe (kg)	Weight of full packed TNT / C4 (kg)	Total weight of casing and steel balls + TNT / C4 (kg)	Bare charge equivalent TNT corresponding to cased TNT / cased C4 (kg)
80	3.2	1.67	1.58 / 1.55	4.59 / 4.56	1.09 / 1.45
100	3.6	2.43	2.87 / 2.81	7.06 / 7.00	2.04 / 2.73
125	5.0	4.15	4.49 / 4.41	10.83 / 10.74	3.15 / 4.22

Similarly if C4 was used as the explosive, the amounts of C4 which can be fully packed in the pipe are 1.55 kg, 2.81 kg and 4.41 kg for the pipe size of 80 mm, 100 mm and 125 mm, respectively. By using Equation 7, they are equivalent to TNT bare charge of 1.45 kg, 2.73 kg and 4.22 kg, respectively. The summary results of cased and bare charges of both TNT and C4 are presented in Table 2.

From the previous FE analyses, the explosive used in this blast incident is equivalent to 3 kg of TNT bare charge. Therefore, one of the possibilities of dimensions and types of explosive is pipe size of 100 mm packed with C4 where the equivalent weights of bare TNT are 2.73 kg. Another possibility of dimension and type of explosive analyzed in this study is pipe size of 125 mm packed with TNT where the weight of bare TNT is 3.15 kg. As previously mentioned, the TNT equivalencies of most other explosives are in between those of TNT and C4 [35], therefore, the diameter of the pipe used in this incident should be still in between 100 mm and 125 mm with the assumed length of 250 mm.

3.3 Lethal radius caused by blast pressure

In order to evaluate the human lethality from explosion, the Bowen lethality curves [27] which consider both blast pressure and duration of explosion are employed in this research. However, the duration of blast in X-axis of the Bowen's curves is converted to the corresponded distance from an equivalent of 3 kg TNT explosion using CONWEP code so that the lethal radius can be determined. The relationship between blast incident pressure – distance at each probability of lethality is shown in Figure 7. The blast incident pressures at some standoff distances are also plotted in this figure. The intersection of incident pressure curve and Bowen's curves yields the corresponding standoff distances for each probability of lethality (see Table 3). The distance corresponded to a 99% lethality can be defined as a lethal radius resulted from this level of explosion. This analysis shows that the lethal radius of this explosion resulted from blast pressure is 2.4 m whilst people stand 5.3 m further from the explosion likely to be safe from blast pressure (see Table 3).

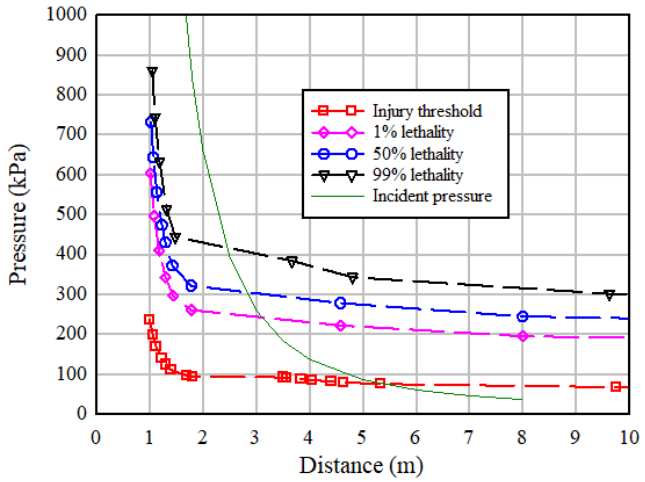

Figure 7 Blast pressure – distance curves corresponded to the each level of probability of lethality

Table 3 Corresponding standoff distances for each level of probability of lethality resulted from blast pressure

Probability of lethality	Distance (m)
Injury threshold	5.3
1% lethality	3.1
50% lethality	2.8
99% lethality	2.4

3.4 Lethal zone caused by blast fragments

In order to determine a lethal zone of the pipe bomb, effects of both natural and preformed fragments have to be considered. Natural fragments are generated from pieces of steel pipe with diameter of 100 mm and thickness of 3.6 mm as analyzed from the previous section. The police officers from the Explosive Ordnance Disposal (EOD) department reported that they collected many steel balls with the diameter about 6 mm around the crime scene [41],[42],[43] as shown in Figure 8. However, the total number of these steel balls as preformed fragments was not reported. Therefore, the analysis of lethal zone in this section is based on the assumption that 6 mm diameter steel balls were distributed on the inner surface of the pipe and around the explosive. As previously stated, a 50% probability of lethality (P_l) is employed to define the boundary of the lethal zone resulted from the explosion of a pipe bomb. However, the fragment hit density has to be determined in order to calculate the probability of lethality. As the fragment hit density decreases when the standoff distance increases, therefore, the calculation of fragment hit density along the distance from the explosion has to be performed. These data are then used to plot the contour line of probability of lethality.

Figure 8 Steel balls collected from the crime scene (photo from [42])

The procedure to determine fragment hit density and probability of lethality starts with calculation of various parameters such as fragment mass distribution (Equations 1 and 2), initial fragment velocity (Equation 3), fragment collision velocity (Equation 4), and spray angle of fragments (Equation 5). These calculations are performed for both natural and preformed fragments. However, the mass distribution of preformed fragment is not required since the assumption of using steel balls with diameter of 6 mm was made earlier. It is noted that the calculation of initial velocity of preformed fragment takes into account of the gas (pressure) leakage between each preformed fragment by introduce the gas reduction factor of 0.5 to the C/M value. All the parameters used in the calculation are presented in Table 4.

Table 4. Parameters used to calculate distribution, velocity and spray angle of fragment, fragment hit density and probability of lethality

	TNT	C4
$\sqrt{2E}$ (m s^{-1})	2,440	2,800
B ($g^{1/2}$ $mm^{-7/6}$)	0.038	0.027
C (kg)	2.87	2.81
V_0 (m s^{-1})	6,800	8,100
M_0 (kg)	2.43	
t (mm)	3.6	
d (mm)	106.7	
ρ_a (kg mm^{-3})	1.225	
	Natural fragment	Preformed fragment
C_D	1.07	0.92

From the calculation performed using Equation 1 and Equation 2, it was found that there are 1,230 natural fragments with weight higher than 0.5 gram while the maximum weight is 11 gram. The total numbers of preformed fragments (6 mm steel balls) which can be placed on the inner surface of the pipe are 1,840.

By using Equation 3, the maximum initial velocities for natural and preformed fragments are 2,000 m s^{-1} and 1,560 m s^{-1}, respectively. Figure 9 shows the detonation point where the cap was embedded into one side of the explosive and the initial velocity vectors of natural fragments along the pipe bomb. The pattern of fragment spray angle is unsymmetrical as a result of one-end detonation of the pipe bomb. It should be noted that the position of detonation point which is also considered in this study mainly affects to the direction of fragments at each location of the pipe bomb.

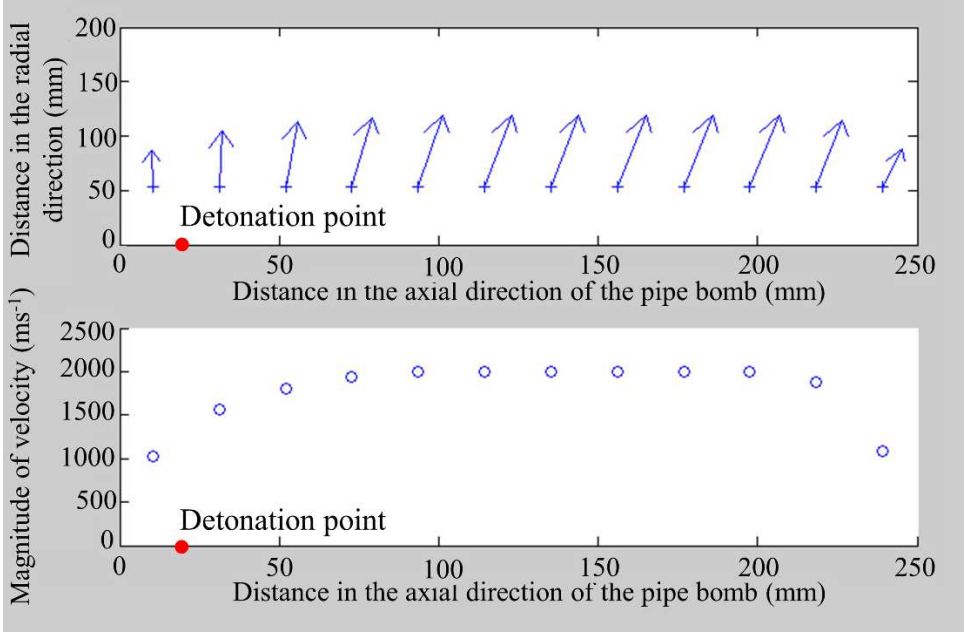

Figure 9 Velocity vectors of fragments from the pipe bomb

Next step is to determine the fragment hit densities at various standoff distances. Figure 10 illustrates the distribution of projected fragments around the center of the explosion. Once fragments hit the target and the corresponded projected area are determined, fragment hit densities at various positions can be obtained. The impact velocities of the fragments at these distances considering air drag forces are also calculated using Equation 4. Then, the kinetic energy of both natural and preformed fragments can be calculated. In order to calculate probabilities of lethality (P_l) at various distances using Equation 6, the criterion of heavy damage level on a person shown in Table 1 is selected. A series of calculation of P_l at various distances were performed systematically using a MATLAB m file code.

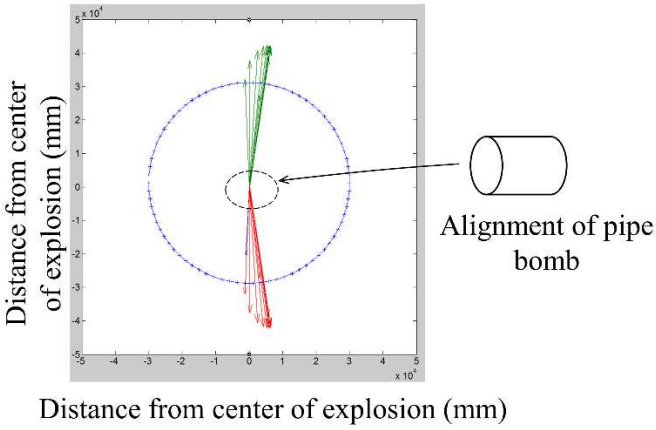

Figure 10 Distribution of projected fragments around center of explosion

The probabilities of lethality (P_l) were calculated for the standoff distances from 1.5 m to 40 m in this study. All the results were used to construct contour lines of P_l values as shown in Figure 11 where the scale shows the P_l from 0.2 to 1.0. It is noted that Figure 11 presents axisymmetry of the P_l contour lines around x-axis. The boundary of lethal zone can be defined using the criterion of 50% of P_l as stated previously; therefore, the contour lines of P_l are limited to the minimum of 0.5. Figure 12 presents the lethal zone resulted from the explosion of the pipe bomb where its boundary is at P_l of 0.5. It can be seen from Figure 12 that the lethal range is about 23 m from the explosion center. People stand outside the radius of 23 m may still suffer some considerable injuries but not to death. Some others stand beyond 35 m from the center of explosion would suffer minor damage as the P_l value is less than 0.2 (see Figure 11). However, it should be reminded that one important factor is the location of a person relative to the alignment of the pipe bomb.

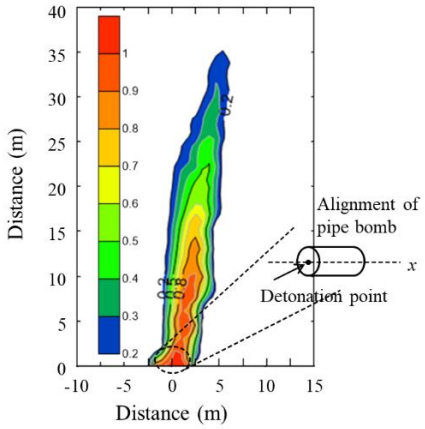

Figure 11 Contours of probability of lethality resulted from fragment impact

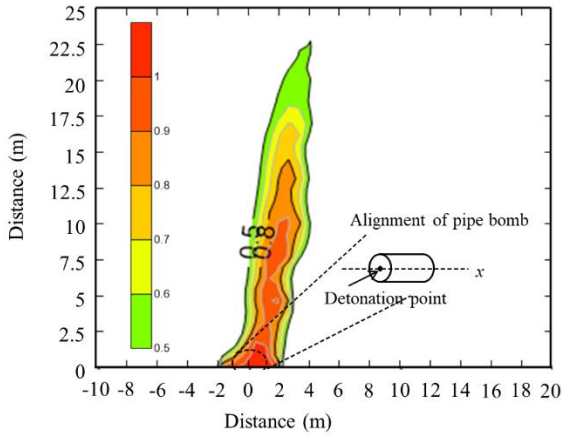

Figure 12 Lethal zone defined by probability of lethality of at least 50%

3.5 Combined lethal zone resulted from blast pressure and fragment impact

Since the lethality can be the results from either blast pressure or fragment impact or from both, the complete lethal zones should then be combined from each of them. The combined lethal zone is presented in Figure 13. The lethal zone with 99% lethality and injury threshold resulted from blast pressure are within a radius of 2.4 m and 5.3 m., respectively, (see Table 3 and Figure 13) around the center of explosion which is obtained when the minimum injury level is eardrum rupture. Figure 13 illustrates how the relative standing position affects damage and/or lethality of a person from pressure and fragment. Zone a, within the radius of 2.4 m, covers the area where both blast pressure and fragment cause human lethality. A person stands less than 5.3 m from the center of explosion but not in the trajectory of flying fragments (Zone b) will be injured from blast pressure whilst if that person stands in the same distance and in the trajectory of fragments (Zone c), the person will be dead by the results of both pressure and fragments. Zone d illustrates that the person may be safe from blast pressure but not from fragments if he/she stands beyond 5.3 m but less than 23 m in the trajectory of flying fragments. Finally, the person will be safe from both pressure and fragments if he/she stands beyond 5.3 m and not in the fragment trajectory as illustrated as Zone e.

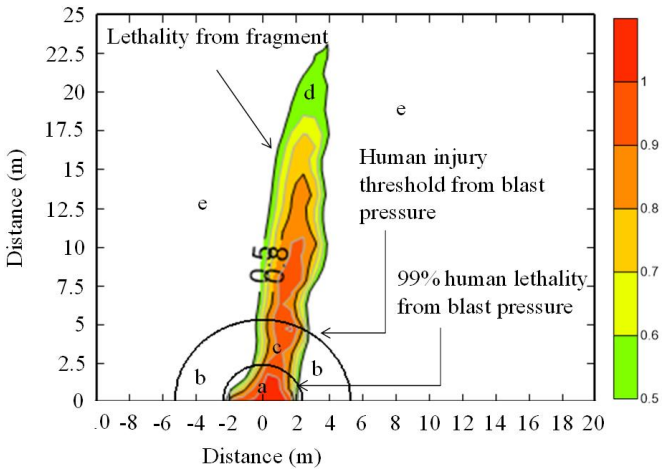

Figure 13 Combined lethal zone resulted from blast pressure and fragment impact

4. Comparison of damage from analysis and actual incident

It was observed from online medias [34],[40],[44] that most of the deaths were in the radius within 3 m from the center of explosion. However, the exact information about causes of lethality whether comes from blast pressure or fragment could not be obtained.

This information is rather consistent with the lethality zone shown in Figure 13 that the damages from pressure and lethality from fragments are within 5 m. Figure 14 shows the nearby distances from the center of explosion. Many evidences [34],[40],[44] show the lethality of persons in the walkway which is within 3m and also inside the shrine fence. Some deaths were found on the street near the walkway. However, a few pedestrians on the traffic island which is around 10 m from the explosion center (see Figure 14) survived from the blast without injury. This is also in accordance with the lethality zone presented in Figure 13. It should be noted that the pedestrians on the traffic island were safe from blast pressure and fragments, although the fragment impact is able to cause lethality at this distance. This circumstance may be resulted from that they were not in the trajectory of flying fragments where this circumstance is represented by Zone e in Figure 13. Another reason is that analysis performed in this research assumes a total of 1,840 preformed fragments whilst there might be less preformed fragments in the pipe bomb. It should be noted that a total of 1,840 preformed fragments is an ideal case of fully packed of 6 mm steel balls between the inner surface of the pipe and the filled explosive. The comparison of actual and analyzed damage levels is summarized in Table 5.

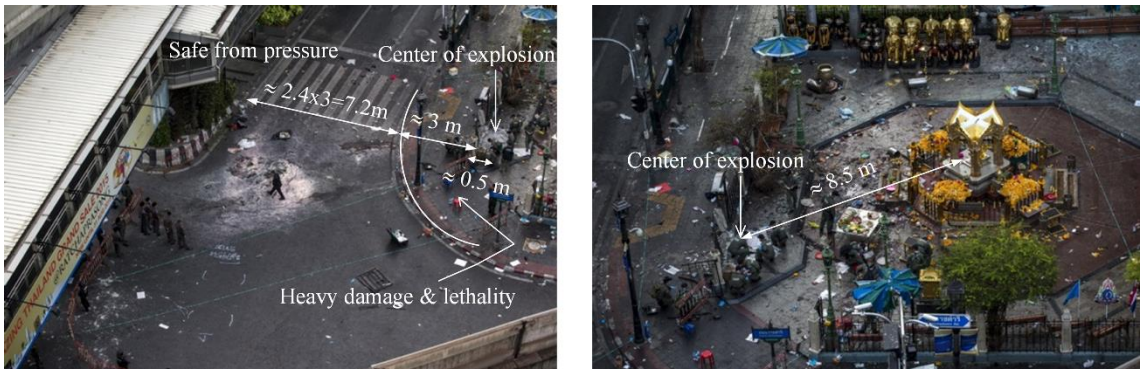

Figure 14 Corresponded distances to actual damage levels on human from the incident scene (photos from [34])

Table 5. Comparison of damage levels from the blast incident

Distance (m)	Damage level from analysis		Observed damage level
	by blast pressure	by fragment[a]	
< 3	High chance of lethality	Lethality	Lethality
3 – 5	Low chance of lethality	Lethality	Severe damage - Lethality
5 - 7.5	Injury threshold	Lethality	Moderate damage - Lethality
7.5 - 10	No damage	Lethality	No damage - Minor damage

Note: [a]People stand inside zone a, c and d (see Figure 13)

5. Analysis of bomb orientation and mapping of the lethal zone on the scene of incident

Further detailed analysis was conducted in order to determine the lethal zone on the scene of incident. The boundary of concrete spalling on the slab was one of the evidence used to predict the alignment of the bomb. Figure 15 shows the possible alignment and position of the bomb, including the location of detonation point. From an investigation of the damage pattern of the slab, it is likely that the bomb axis is around 10° counterclockwise from the fence alignment. It can be seen that the damage area of concrete slab was more severe in the radial direction of the bomb compared to that near both ends of the bomb. This is due to the fact that the cylindrical charge of which length to diameter is greater than 1 produces higher blast pressure in the radial direction compared to that produced at the ends of the cylindrical charge [46]. The alignment of the bomb and location of the detonation point shown in Figure 15 was proven by investigation of the contour of blast pressure and the damage pattern on the slab resulted from 3D Arbitrary Lagrange Euler (ALE) FE analysis where the bomb was modeled in a full 3D cylindrical shape (ϕ=100mm and L=250mm). The TNT explosive was modeled using Jones-Wilkins-Lee (JWL) equation of state [47]. Euler element formulation was employed to model explosive and surrounded air domain whereas the concrete slab was modelled using Lagrange element formulation. It is noted that the effects of shape of explosive and interaction between explosive

and structures can be included by using this analysis technique. However, this kind of analysis takes much of computer resources especially when the analysed domain is large. This research employed ANSYS AUTODYN [48] to perform ALE analyses only to investigate the possible alignment of the bomb used in the incident. Only the explosive, air and concrete slab were modelled in this section. Figure 16 shows the detonation point and alignment of the bomb where its axis is 10° counterclockwise from the fence similarly to that presented in Figure 15. Figure 16 also shows the contours of blast pressure resulted from the explosion of the cylindrical charge. It can be seen that blast pressure is rather high in the radius direction compared to that in the longitudinal direction. This pattern of blast pressure results in the pattern of slab damage as presented in Figure 17 which is similar to that observed from the actual blast incident (see Figure 15). The predicted area of spalled RC slab from the ALE analysis is 0.558 m^2 whilst the actual damaged area of slab is calculated and estimated from Figure 15 is 0.546 m^2.

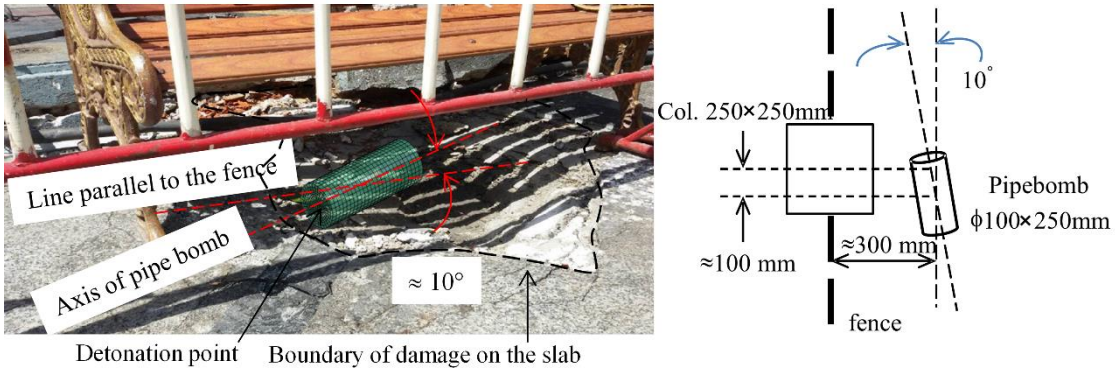

Figure 15 Possible alignment and position of pipe bomb (photo from Than Tao Mahaprom Foundation)

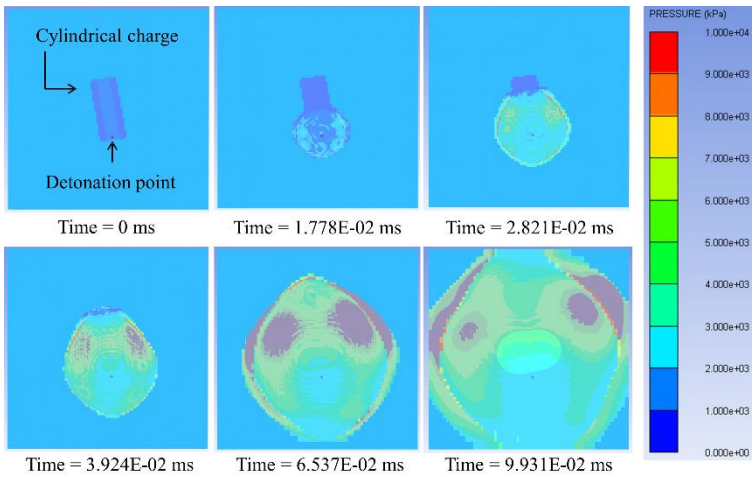

Figure 16 Contour of blast pressure from explosion of the pipe bomb (ϕ=100 mm and L=250 mm)

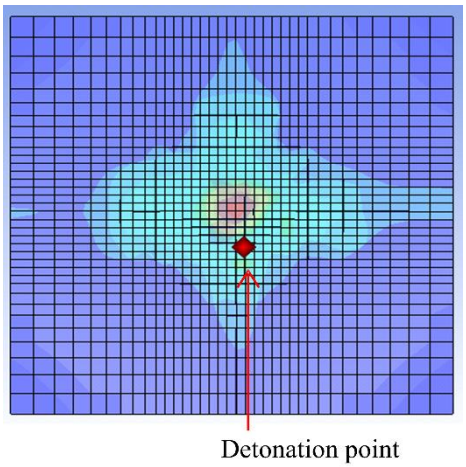

Figure 17 Pattern of slab damage

After the alignment of the bomb and the location of detonation point were verified using the ALE-FE model, the lethal zone in Figure 13 can be mapped on the drawing of the Erawan shrine. The axis of the bomb is set to 10° counterclockwise from the fence alignment. The lethal zone resulted from the fragment impact is concentrated in the perpendicular direction to the axis of the pipe bomb because the ejection of fragments occurs in the radial direction of the bomb with some fragment spray angles as shown in Figure 9. Figure 18 shows the lethal zone obtained from blast pressure and fragment impact on the plan view of the Erawan shrine. It can be seen that Than Tao Mahaprom statue is in the lethal zone resulted from fragment impact which agrees well with the reported evidences that the statue was hit by a fragment as shown in Figure 18.

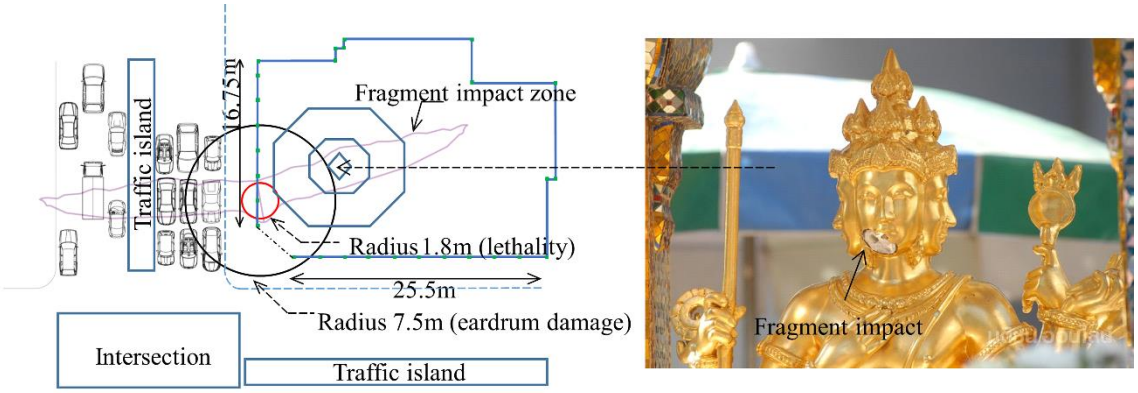

Figure 18 Lethal zone from blast pressure and fragment on the scene of incident (photo from [34])

6. Conclusion

This article aims to employ forensic engineering techniques to analyse a bombing incident. Analysis results are expected to be useful for security authorities in order to obtain more insight about the incident. The concept of analysis is summarized in this article and employed to analyse one case study which is the explosion at Erawan shrine in Bangkok, Thailand. The analysis starts with the determination of possible weight of equivalent bare TNT by FE analyses of RC fence structure of the shrine. The sophisticated constitutive material models of concrete and steel

reinforcement taken into account of strain rate effects are included in the FE models. The possible charge weight can be obtained by comparing the damage levels of the models to the actual damage level observed from the scene of incident. Then, the possible size of pipe bomb used in the incident is determined based on the formulation which relates bare and cased charge weight.

Injury levels and lethality of person are also assessed in this article. Both blast pressure and fragment impact are considered to define the boundary of lethal zone caused by an explosion of pipe bomb. The analyzed lethal zone mapped on the plan view of the shrine is then compared with the actual damage level and lethality of persons observed in the actual incident. Although only limited information was open to public, analysis results agree reasonably well with the actual observed damage level. The proposed forensic engineering technique can be employed to plan and manage the security policy for each specific community to ensure the community safety. Last but not least, the authors would like to express deep consolation to all lost from this incident.

Acknowledgment

The authors would like to gratefully acknowledge Than Tao Mahaprom Foundation, and the Erawan Hotel for sharing information and photos of damage at the Erawan Shrine after the explosion incident.

Declarations

The authors received the financial support from the Center of Excellence in Material Science, Construction and Maintenance Technology, Thammasat University and the Higher Education Research Promotion and National Research University Project of Thailand, Office of the Higher Education Commission. This study was also financially supported by the Chair Professor Grant (P-19-52302), The National Science and Technology Development Agency (NSTDA). The authors also declare that they have no personal relationships that could have appeared to influence the work reported in this paper.

References

[1] American Society of Civil Engineers (ASCE). (2016). “Forensic Engineering.” ⟨http://www.asce.org/forensic-engineering/forensic-engineering⟩ (May. 16, 2016).

[2] Zineddin, M., & Krauthammer, T. (2007). Dynamic response and behavior of reinforced concrete slabs under impact loading. International Journal of Impact Engineering, 34(9), 1517-1534.

[3] Task Committee. (1999). Structural Design for Physical Security: State of the Practice. ASCE.

[4] Wu, C., Oehlers, D. J., Wachl, J., Glynn, C., Spencer, A., Merrigan, M., & Day, I. (2007). Blast testing of RC slabs retrofitted with NSM CFRP plates. Advances in Structural Engineering, 10(4), 397-414.

[5] Wu, C., Oehlers, D. J., Rebentrost, M., Leach, J., & Whittaker, A. S. (2009). Blast testing of ultra-high performance fibre and FRP-retrofitted concrete slabs. Engineering structures, 31(9), 2060-2069.

[6] Tanapornraweekit, G., Haritos, N., Mendis, P., & Ngo, T. (2010). Finite element simulation of FRP strengthened reinforced concrete slabs under two independent air blasts. International Journal of Protective Structures, 1(4), 469-488.

[7] Tanapornraweekit, G. (2010). Behavior of fiber reinforced polymer (FRP) strengthened RC slabs subjected to blast loading, Ph.D. Thesis, University of Melbourne.

[8] Tanapornraweekit, G., Haritos, N., & Mendis, P. (2011). Behavior of FRP-RC slabs under multiple independent air blasts. Journal of Performance of Constructed Facilities, 25(5), 433-440.

[9] Ha, J. H., Yi, N. H., Choi, J. K., & Kim, J. H. J. (2011). Experimental study on hybrid CFRP-PU strengthening effect on RC panels under blast loading. Composite Structures, 93(8), 2070-2082.

[10] Li, J., & Hao, H. (2014). Numerical study of concrete spall damage to blast loads. International journal of impact engineering, 68, 41-55.

[11] Li, J., Wu, C., & Hao, H. (2015). Investigation of ultra-high performance concrete slab and normal strength concrete slab under contact explosion. Engineering Structures, 102, 395-408.

[12] Li, J., Wu, C., Hao, H., & Su, Y. (2017). Experimental and numerical study on steel wire mesh reinforced concrete slab under contact explosion. Materials & Design, 116, 77-91.

[13] McVay, M. K. (1988). Spall damage of concrete structures. ARMY Engineer Waterways Experiment Station Vicksburg MS Structures LAB.

[14] Mao, L., Barnett, S., Begg, D., Schleyer, G., & Wight, G. (2014). Numerical simulation of ultra-high performance fibre reinforced concrete panel subjected to blast loading. International Journal of Impact Engineering, 64, 91-100.

[15] Hao, H., Hao, Y., Li, J., & Chen, W. (2016). Review of the current practices in blast-resistant analysis and design of concrete structures. Advances in Structural Engineering, 19(8), 1193-1223.

[16] Biggs, J. M. (1964). Introduction to Structural Dynamics, McGrawHill Inc. New York, New York.

[17] Mays, G. & Smith, P. D. (1995). Blast effects on buildings: Design of buildings to optimize resistance to blast loading. Thomas Telford.

[18] Hao, H. (2015). Predictions of structural response to dynamic loads of different loading rates. International Journal of Protective Structures, 6, 585-605.

[19] Hallquist, J. O. (2016). LS-DYNA theory manual R9. 0. Livermore Software Technology Corporation, Livermore.

[20] Abeysinghe, T. (2017). Behaviour of internal and external fiber reinforced concrete panels under blast load, MSc. Thesis, Thammasat University.

[21] Malvar, L. J., Crawford, J. E., & Morrill, K. B. (2000). K&C concrete material model release III-automated generation of material model input. Karagozian and Case Structural Engineers, Technical Report TR-99-24.3.

[22] Malvar, L. J., Crawford, J. E., Wesevich, J. W., & Simons, D. (1997). A plasticity concrete material model for DYNA3D. International journal of impact engineering, 19(9-10), 847-873.

[23] Tu, Z., & Lu, Y. (2009). Evaluation of typical concrete material models used in hydrocodes for high dynamic response simulations. International Journal of Impact Engineering, 36(1), 132-146.

[24] Tan, S. H., Chan, R., Poon, J. K., & CHNG, D. (2014). Verification of concrete material models for MM-ALE simulations. 13th International LS-DYNA User's Conference.

[25] Xu, K., & Lu, Y. (2006). Numerical simulation study of spallation in reinforced concrete plates subjected to blast loading. Computers & Structures, 84(5), 431-438.

[26] Tang, E. K., & Hao, H. (2010). Numerical simulation of a cable-stayed bridge response to blast loads, Part I: Model development and response calculations. Engineering Structures, 32(10), 3180-3192.

[27] Bowen I G, Fletcher E R, Richmond D R, Estimate of Man's Tolerance to the Direct Effects of Air Blast, Technical Progress Report, DASA-2113, Defense Atomic Support Agency, Department of Defense,Washington, DC, October 1968

[28] Mott, N. F. (1943). A Theory of the Fragmentation of Shells and Bombs, Ministry of Supply. AC4035.

[29] Charron, Y. J. (1979). Estimation of velocity distribution of fragmenting warheads using a modified Gurney method, Air Force Institute of Technology, Ohio.

[30] Cooper, P. W. (1996). Explosives engineering, Wiley-VCH.

[31] Campbell, F.P. (1962) "Engineering design handbook - Elements of terminal ballistics-part one: Introduction, kill mechanics and vulnerability" Rep. No. 706-160, U.S. Army Materiel Command, Washinton DC.

[32] Johnson, D. (2002). "AAAV 30 mm HE lethality testing, test procedures and casualty models." 37th Annual Gun & Ammunition Symp. & Exhibition, NAVSEA, Dahlgren, Virginia

[33] Federation of American Scientists (FAS). (1998). “Introduction to Naval Weapons Engineering.” ⟨http://www.fas.org/man/dod-101/navy/docs/es310/dam_crit/dam_crit.htm⟩

[34] ASTV Manager online. (2015). “International news reveals ‘Tourists shocked’ by Ratchaprasong bomb.” ⟨http://www.manager.co.th/Around/ViewNews.aspx?NewsID=9580000093369&Html=1&TabID=1&%20ASTV%20Manager%20Online⟩

[35] US Department of Defense. (2008). Structures to resist the effects of accidental explosions. UFC 3-340-02.

[36] Malvar, L. J., & Crawford, J. E. (1998). Dynamic increase factors for concrete Naval Facilities Engineering Service Center Port hueneme CA. CA.[35]

[37] Marvar, L. J., & Crawford, J. E. (1998, August). Dynamic increase factors for steel reinforcing bars. In Proceedings of the Twenty-Eighth Department of Defense Explosives Safety Seminar. 18-20 Aug.

[38] Post Today. (2015). “Example of ‘Pipe bomb’ at Ratchaprasong ” ⟨http://www.posttoday.com/⟩

[39] Crowley, A. B. (2006). The effect of munition casings on reducing blast overpressures. Gas, 100, M21.

[40] Kapook News. (2015a). “Video footage of the terrorist at Ratchaprasong bomb.” ⟨http://hilight.kapook.com/view/125147⟩

[41] Isranews. (2015). “Explosion at Ratchaprasong road.” ⟨https://www.isranews.org/isranews-article/item/40670-believe_40670.html⟩

[42] Thai news agency. (2015). “Scatttered fragments from the explosion.” ⟨http://www.tnamcot.com/content/261520⟩

[43] Thairath. (2015). “Ratchaprasong bomb compared with 8 other bombing incidents which occurred in Thailand.”⟨http://www.thairath.co.th/content/519135⟩

[44] Khaosod. (2015). “12 dead and many injured from the bombing incident at Ratchaprasong in Erawan shrine.” ⟨http://www.khaosod.co.th/view_newsonline.php?newsid=1439814171⟩

[45] Kapook News. (2015). “20 dead and 130 injured at Ratchaprasong bomb.” ⟨http://hilight.kapook.com/view/125171⟩

[46] Plooster, M. N. (1982). “Blast effects from cylindrical explosive charges: Experimental measurements.” Rep. No. ADA121863, Denver Research Institute, Naval Weapons Center, California.

[47] Dobratz, B. M., & Crawford, P. C. (1985). LLNL explosives handbook. UCRL-52997 Rev, 2.

[48] ANSYS AUTODYN user manual Version 4.3. (2005). Century Dynamics Inc., Concord, California.